RSC Advances

ROYAL SOCIETY OF CHEMISTRY

www.rsc.org/advances

Journal Name

ARTICLE

Synthesis and characterization of solvent-free waterborne polyurethane dispersion with both sulfonic and carboxylic hydrophilic chain-extending agents for matt coatings application

Received 00th January 20xx,
Accepted 00th January 20xx

DOI: 10.1039/x0xx00000x

www.rsc.org/

Qiwen Yong,[a,b] Fuwei Nian,[a,c] Bing Liao,[d] Liping Huang,[a,b] Lu Wang,[a,b] Hao Pang,[a,†]

Simultaneously using sulfonic and carboxylic acid as hydrophilic chain-extending agents, a new type of solvent-free and chemical matt waterborne polyurethane resin was prepared and investigated. The chemical structure containing t.. urethane and urea groups in this novel carboxylate/sulfonate type of waterborne polyurethane (CSWPU) resin w.. confirmed by FTIR, ^{1}H and ^{13}C NMR spectra. An obvious advantage for the environment is that, unlike the traditional synthetic method for waterborne polyurethane, the reactive system needn't any organic solvent to reduce the viscosity of prepolymer in the process of prepolymerization. In addition, the gloss extinction was generated by the drying process o.. the resin itself, without the requirement of any matting agents. 3D-AFM images indicate that the surface of the matt CSWPU films was extremely rough and was comprised of many spherical particles with the diameter in the range of 0.8 .. 3.0 μm arranging on the films' surface. The well matt CSWPU resin tended to have a relatively higher molecular weight and lower swelling ratio. Moreover, an increase of sulfonic hydrophilic chain-extending agent content or the initial molecula.. weight of the soft segment facilitated the improvement of thermal stability.

Introduction

With the change of people's aesthetic ideas, matt coatings are more and more popular in the decoration of surfaces[1]. Such surfaces, when incorporated into commercial products such as leathers, fabrics, and papers, could produce a very natural optical appearance, pleasant haptic, and seemed to be suitable for masking minor scratches, dust build-up, and fingerprints[2–5]. The phenomenon of matting has a great relationship with the ability of the coating's surface to reflect light. A high gloss surface would reflect most of the light received while the matt surface would mainly produce internal refraction and abortion to the incident light instead of reflecting it[6–8].

The traditional method of extinction is to add a variety of fillers into the polyurethane or acrylic resin, which are known as physical extinction. The fillers are developed from the natural diatomite[9,10] to wax micropowder[11] and then to synthetic silica gels[12,13], as well as organic polymer fillers[14]. There are many disadvantages to this method which are listed below. First, the precipitation of the matting agent may easily cause uneven mixing before painting, thus leading to a different gloss level of the coating's surface. Second, the matting agent and resin are incompatible to some extent, so the coating is easy to chalk and be peeled off. The specular gloss degree is also likely to rise over the times. Finally, the condensation of the composition tends to produce many-seeded appearance and be lack of a soft surface feeling by touch[15–18].

Considering the lack of studies in the existing literatures on the chemical extinction of waterborne polyurethane (WPU) resin, an enormous amount of research effort goes into the chemical matt technology. A new kind of chemical matt waterborne polyurethane resin with both sulfonic and carboxylic hydrophilic chain-extending agents, such as 2, 2-Bis (hydroxymethyl) propionic acid (DMPA), and the other was sodium 2-[(2-amino ethyl) amino] ethane sulfonate (SAAS), was fabricated. Currently, most of the WPU resin in the market is classified into the carboxylate type, sulfonate type is rarely to be seen, not to mention the waterborne polyurethane resin combining both of them. However, excessive use of DMPA will decrease the hardness and water resistance of WPU coatings while SAAS can offer hydrolytic stability and thermal stability of coatings better than the use of DMPA[19–21]. More importantly, SAAS is able to make WPU emulsions form a lot of stereoregular spherical particles, which is of great significance to produce a matt effect. Furthermore, this novel carboxylate/sulfonate type of waterborne polyurethane (CSWPU) resin needn't any organic solvent, which is highly beneficial to the environment. Because a quite high R (the molar ratio of NCO/OH) value used means a large excess of isophorone diisocyanate (IPDI) was not only served as reactant, but also served as a solvent in the prepolymer process.

[a] Key Laboratory of Cellulose and Lignocellulosics Chemistry, Guangzhou Institute of Chemistry, Chinese Academy of Sciences, Guangzhou 510650, China
[b] University of Chinese Academy of Sciences, Beijing 100049, China.
[c] Guangzhou Green Building Materials Academy, Guangzhou Institute of Chemistry, Chinese Academy of Sciences, Guangzhou 510650, China
[d] Guangdong Academy of Sciences, Guangzhou 510650, China
† Corresponding author at present address: Guangzhou Institute of Chemistry, Chinese Academy of Sciences, Guangzhou 510650, China. E-mail: panghao@gic.ac.cn. Tel. /fax: +86 020 85231236.

In the present study, we successfully synthesized a new solvent-free waterborne polyurethane dispersion with both sulfonic and carboxylic hydrophilic chain-extending agents for matt coatings application, which didn't require any organic solvent in initial stage to lower the viscosity of prepolymer. ATR-FTIR, ^{1}H and ^{13}CNMR were used to characterize the chemical structure as well as various hydrogen bonds of CSWPU film, 3D-AFM and TEM were employed to observe the surface profiles and particle size distribution analysis, elaborating the matt mechanism of this novel CSWPU film without the addition of any extra matting agents. The properties such as molecular weight (by GPC), the degree of gloss, thermal performance (by TGA), and average swelling ratio were also evaluated. By adjusting the SAAS content, CSWPU resin with different gloss levels was synthesized. The effect of different molecular weight of the polyols on the thermal resistance and the specular gloss levels were also investigated.

Materials and methods

Materials

Polytetramethylene ether glycols (PTMEG, 2000 and 1000 g/mol) purchased from Aladdin Reagent was dried at 80 °C under vacuum for 10 h before use. 2, 2-Bis (hydroxymethyl) propionic acid (DMPA) also provided by Aladdin Reagent was dried at 60 °C for 6 h under vacuum. Isophorone diisocyanate (IPDI, Aladdin Reagent), dibutyltin dilaurate (DBTDL, Sinopharm Chemical Reagent), trimethylamine (TEA, Sinopharm Chemical Reagent), sodium 2-[(2-amino ethyl) amino] ethane sulfonate (SAAS salt, Quzhou Mingfeng Chemicals, China) and hydrazine hydrate (HHA, Sinopharm Chemical) were used as received.

Synthesis of carboxylate type of prepolymer

CSWPU resin was synthesized by two steps of step-growth polymerization. PTMEG with different molecular weight (Mn) 1000 or 2000 were used as the soft segment. It was first added to the vessel and stirred for 30 min. Prepolymerization was carried out at approximately 80 °C by adding a large excess of IPDI under nitrogen atmosphere for 2 h in the presence of DBTDL as the catalyst (0.05 ml). Then DMPA was added to the reactor under reflux for 2 h. After the system cooled to 40 °C, Triethylamine was fed into the reactor to neutralize the carboxylic groups for 30 min. The stoichiometric ratio of PTMEG / IPDI / DMPA / TEA was 9.1:3.6:1:1. All reagents without specified instructions were supplied by Shanghai Aladdin and used as received.

Synthesis of matt carboxylate and sulfonate type of WPU

The carboxylic acid prepolymer with the different contents of SAAS were obtained. The SAAS was diluted with a small amount of deionized water and was added to the reactor under vigorous stirring at 40 °C for 30 min. Then a large amount of deionized water was fed into the vessel to dilute to a certain solid content under vigorous stirring for 30 min. The final chain extension was carried out with a solution of hydrazine hydrate. Determination of the end of the reaction was observed by examining the absorption band of isocyanate groups in the range of 2270 cm^{-1} being disappeared, typically lasting for 1 h. The CSWPU resin was designated as the weight ratio of DMPA to SAAS in both hydrophilic chain-extending agents. The sample marked as, for example, D60S40, means that the content of DMPA is 60 wt% and 40 wt% SAAS in both hydrophilic chain-extending agents as shown in Table 1.The solid content was about 30 %.

Table 1 Designations and the specular gloss levels of CSWPU resins*

Sample	Soft segment	Abbreviation	Weight ratio (wt%)		Gloss levels (°)
			DMPA	SAAS	
CSWPU1	PTMEG 1000	D60S40	60	40	24
CSWPU2		D50S50	50	50	6
CSWPU3		D40S60	40	60	41
CSWPU4	PTMEG 2000	D50S50	50	50	10

*The weight of DMPA is fixed at all samples.

Preparation of CSWPU films

CSWPU films were prepared by pouring the aqueous resins onto a Teflon plate (10 × 10 cm) and dried at an ambient temperature for 5 days, and then vacuum dried at 60 °C for 24 h[22,23]. After that they were peeled off from the Teflon plate. The dried films were stored in a desiccator.

Chemical structure characterization

ATR-FTIR measurement of CSWPU film was carried out on a Bruker Tensor 27 FTIR spectrometer under N_2 purging and was scanned 16 times at a resolution of 1 cm^{-1} over the frequency range of 4000 ~ 600 cm^{-1}. ^{1}H and ^{13}C NMR spectra of CSWPU films were recorded on a Bruker DRX-400 spectrometer with $CDCl_3$ as the solvent. Tetramethylsilane was used as an internal reference. 3D surface morphology observation of CSWPU films was performed with atomic force microscope (AFM, Bruker Multimode 8). The scanning rate was 0.5 Hz and all the measurements were carried out using ScanAsyst mode AFM technique.

Physical properties of CSWPU films

Molecular weight was determined by a gel permeation chromatography (GPC) with polystyrene calibration using a Perkin Elmer series 200 HPLC system equipped with Jordi Gel DVB column at 35 °C in tetrahydrofuran. CSWPU resins were examined by TEM (JEM 100CXII) using 100 kV electron beam. The CSWPU resins were first diluted to 500 ppm, and then stained by 2 wt% phosphotungstic acid for 10 min before the examination. A portable glossmeter (KGZ-60, Tianjin Yaxing) was used to measure the specular gloss levels. All of the measurements were carried out using the 60 ° incidence angle. The swelling ratios of the films were obtained by the following equation. W_d equals the weight of

dry films, and W_w equals the weight of swollen films which were immersed into the deionized water at room temperature for 24 h and removed the excessive surface water[24,25].

$$\text{Swelling ratio}(\%) = (W_w - W_d) / W_d \times 100\ \%$$

Three samples for each type of WPU and three test specimens obtained from each sample were used to test the swelling properties.

Thermal properties of CSWPU films

Thermal stability was evaluated with a PE pyris 1 TGA analysis under nitrogen flow (10 $cm^3 \cdot min^{-1}$). The samples (2-3 mg) were heated from 50 to 600 °C with heating rate of 10 °C · min^{-1}. The weight loss and its first derivative weight have been recorded simultaneously as a function of temperature.

Results and discussion

Structural characterization of CSWPU resin by FTIR

The structure of CSWPU resin was identified by IR spectroscopy as shown in Figure 1. The absence of a characteristic band at 2270 cm^{-1} (NC=O stretching) indicated that all of the isocyanate groups were reacted in this system[22]. The absorption band at 3530 cm^{-1} (O-H stretching) from PTMEG and DMPA also disappeared. However, the characteristic bands of CSWPU resin centred at 3320 cm^{-1} (N-H stretching) and 1533 cm^{-1} (N-H deformation) emerged in this spectrum[26]. The bands at 2941 cm^{-1} and 2854 cm^{-1} were corresponding to C-H stretching vibration and 2796 cm^{-1} was attributed to the O-CH_2 stretching vibration. The absorption band at 1702 cm^{-1} was attributed to C=O stretching vibration. The small band at 1043 cm^{-1} was assigned to the symmetric stretching mode of –SO_3–, indicating that the SAAS was successfully incorporated into this polymer. The more detailed assignments of characteristic FTIR bands are listed in Table 2.

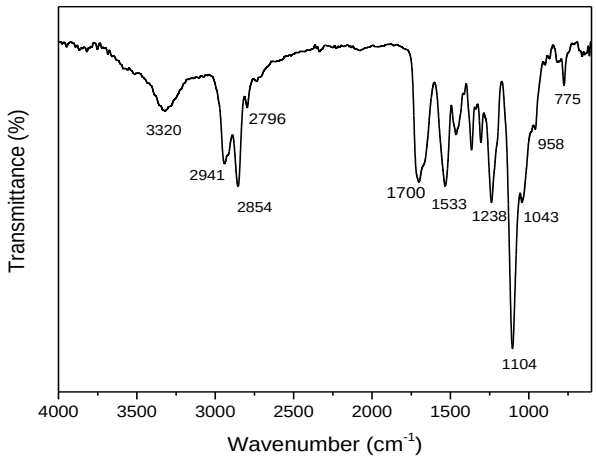

Figure 1. The ATR-FTIR spectrum of CSWPU resin

Table 2 The ATR-FITR bands of the CSWPU resin

Wavelengths (cm-1)	Assignments
3320	ν N-H (free and bonded)
2941,2854	ν C-H (CH, CH_2 and CH_3)
2796	ν O-CH_2
1702	ν C=O (urethane)
1659	ν C=O (urea)
1533	ν C-N + δ N-H
1455	δ CH_2 + δ asym CH_3
1367	δ sym CH_3
1238	ν asym N-CO-O + ν C-O-C
1104, 958	ν C-O-C + ν sym N-CO-O +ν C-C
1043	ν (-SO_3)
770	δ -$(CH_2)_4$

Structural characterization of CSWPU resin by ^{1}H and ^{13}C NMR

The chemical structures of the CSWPU were also verified by the ^{1}H and ^{13}C NMR spectra. The ^{13}C NMR spectra of PTMEG, IPDI and CSWPU film in $CDCl_3$ are shown in Figure 2a, 2b and 2c, respectively. From three pictures, it can be observed that they all have the same triple resonances at about 76.7 ppm, 77.0 ppm and 77.3 ppm where the characteristic signal is from the $CDCl_3$ solvent. Figure 2b has the characteristic resonances at 122.8 and 121.9 ppm, which is not existed at Figure 2c. This indicates that diisocyanate groups were completely reacted. This result was also confirmed by the FTIR analysis. Besides, the signals at 157.3 and 156.0 ppm (the screenshot of Figure 2c) are corresponding to the C=O from urethane and urea groups, respectively. The resonance at 17.6 ppm in Figure 2c is neither originated from Figure 2a nor from Figure 2b, but stemming from the -CH_3 of DMPA. Because the -CH_3 of DMPA was surrounded by a large number of electron clouds and the shielding effect increased, leading to the chemical shift moving to a higher field. The resonance at 23.2 ppm (Figure 2c) is attributed to the three -CH_3 of IPDI. Comparing Figure 2c with Figure 2a, it can be concluded that two strong and sharp resonance located at 26.4 and 70.5 ppm, and the signal at 64.7 ppm correspond to the PTMEG soft segment carbons. In the range of 31.8~54.8 ppm, the signals are partly from the skeleton carbon atoms of IPDI, partly from the DMPA and SAAS. It's difficult to define exactly what each resonance is attributed to, thus the introduction of ^{1}H NMR spectra combined with the ^{13}C NMR spectra is necessary to explore further the specific chemical structure.

Figure 3a, 3b, and 3c show the ^{1}H NMR spectra of PTMEG, IPDI, and CSWPU, respectively. The signals at 7.26 ppm in three pictures are assigned to the protons of $CDCl_3$ solvent. The singlet at 0.7[illegible] and 0.72 ppm can be ascribed to the -CH_3 groups of IPDI and the clear singlet at 1.25 ppm is due to free methyl groups of DMPA. The resources between 0.88 ppm and 1.44 ppm are associated with the partly IPDI protons. Comparing the Figure 3a with Figure 3c, the two strong resonances at 1.65 and 3.41 ppm and the signal at 2.17 ppm are corresponding to the soft-segment protons of PTMEG. The resonances in the range of 2.91~4.06 ppm, except the

strong and sharp signals at about 3.41 ppm, are sophisticated and are partly assigned to the protons of IPDI, and partly assigned to DMPA protons connecting the hydroxyl groups. The new emerging resources at 6.88 ppm and 7.00 ppm are for urea and urethane groups respectively, which were also identified by the ^{13}C NMR analysis. The resonance at 7.52 ppm confirms the presence of NH allophanate group[27,28]. Because of a large excess of IPDI in the system, it was possible for urethane to continue to react with isocyanate groups.

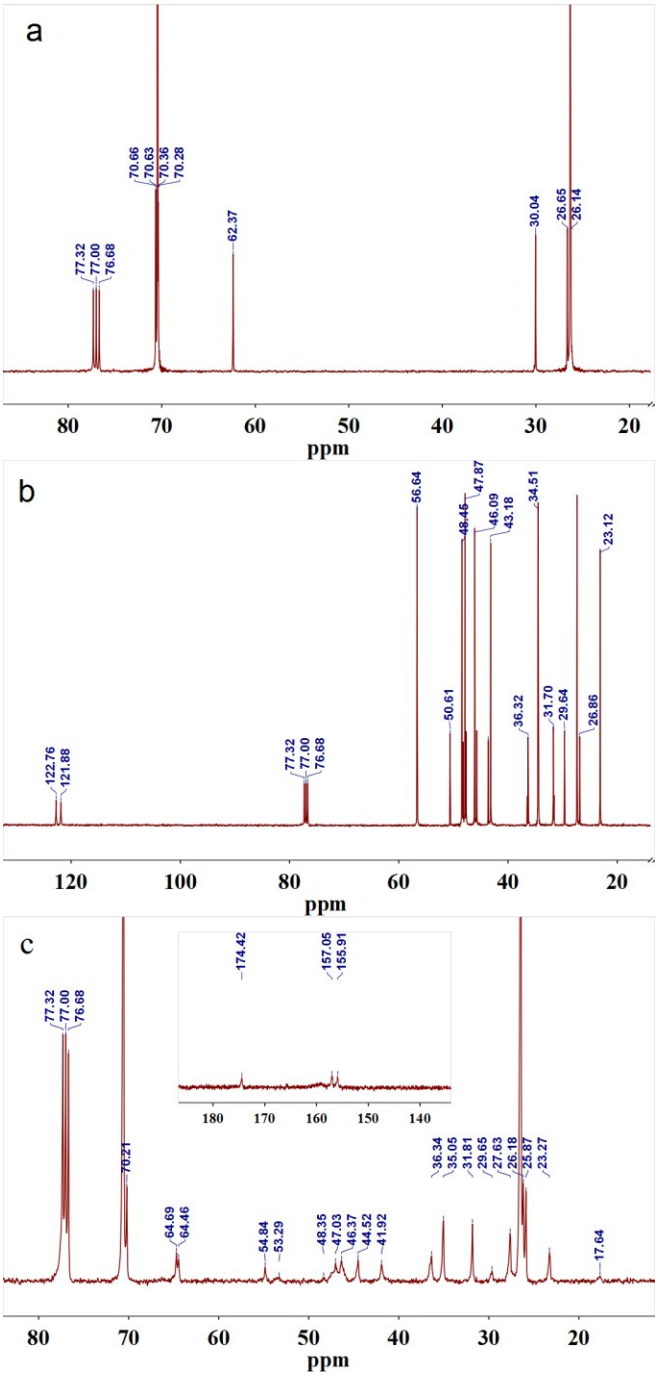

Figure 2. ^{13}C NMR spectra of PTMEG (a), IPDI (b) and CSWPU film (c) in $CDCl_3$

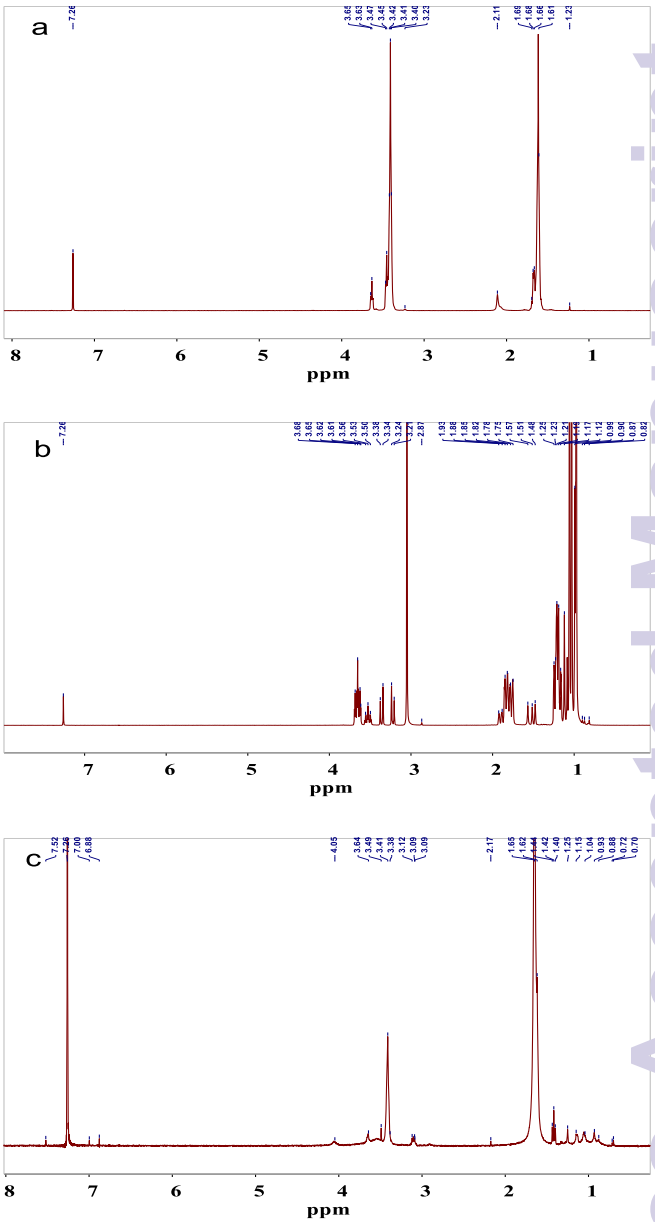

Figure 3. ^{1}H NMR spectra of PTMEG (a), IPDI (b) and CSWPU film (c) in $CDCl_3$

Surface analysis of CSWPU films by AFM

Figure 4 presents the height- and mixed-3D AFM images of CSWPU2 and CSWPU3 films. The scope of the observation was 20×20 μm^2. The mixed-3D AFM images are closer to the authentic superficial structures of the films. The CSWPU2 film surface was very rough, accompanied with many wrinkled spherical particles on it. However, the CSWPU3 film had a very flat and smooth surface morphology. In terms of coordinate axis data, the Z-a value of the CSWPU2 was 592.5 nm, which was far greater than the CSWPU3's Z-axis value 104.3 nm. It means that bulks of wave-crests and wave-troughs of CSWPU2 film made the incident light bend heavily or even be absorbed, and the diffuse radiation occurred. Finally, the matt effect of the CSWPU was achieved. In contrast, the CSWPU3 film was plain, the incident light mainly

reflected on the surface, causing a relatively high specular gloss level of the film.

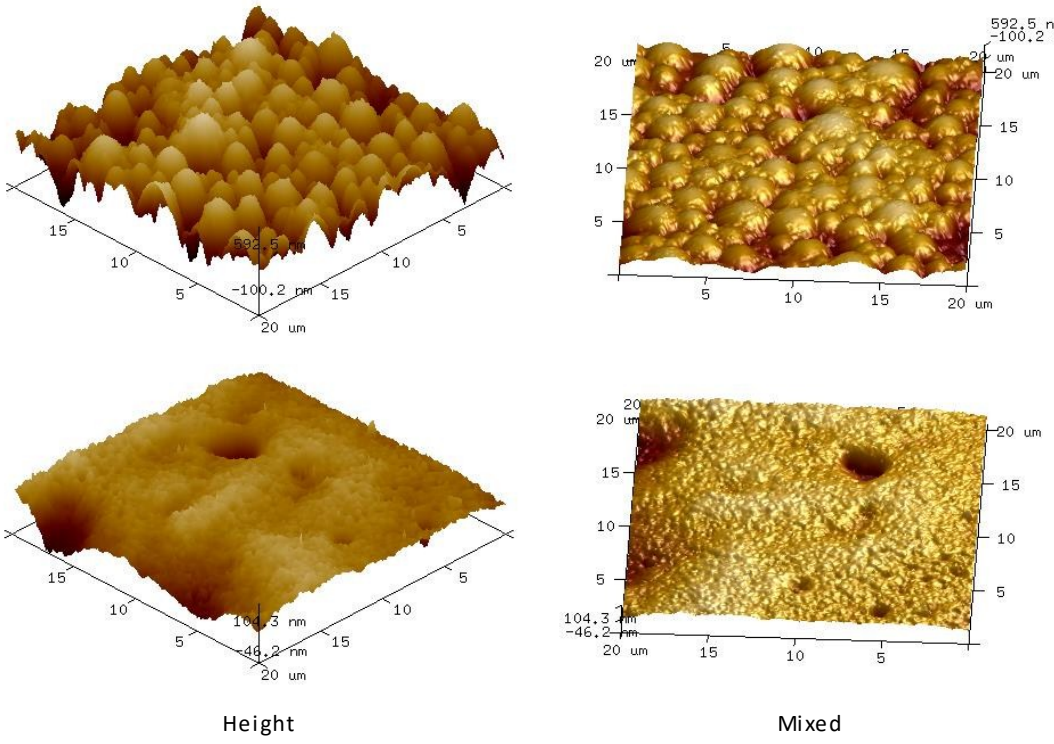

Figure 4. 3D images of CSWPU2 (upper) and CSWPU3 (lower) films

Figure 5 shows the size of individual partides on the surface of the CSWPU2 film. Section analysis in AFM was used to measure the diameter of the spherical partides. One large and one small size of spherical partide were chosen in this range of picture to evaluate the partide diameter and its height. The smaller spherical partide (two red across) diameter is 0.91 µm and the height is -130 nm. The larger one (two blue across) is of diameter 3.54 µm and height of 134 nm. It can be concluded that the well matt CSWPU2 film was due to the formation of numerous spherical partides on its surface. The wide range of partide size distribution was approximately between 0.80 µm and 3.0 µm. In this range of diameters, the light scattering ability of the film is quite strong, hence the gloss degree keep at very low level.

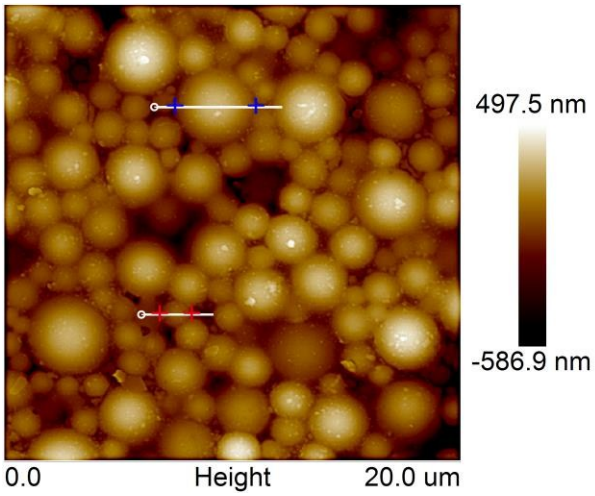

Figure 5. 2D-mixed AFM image of CSWPU2 film

Molecular weight measurements of CSWPU films by GPC

GPC measurements reveal the trend in molecular weight values with the changing weight ratio of DMPA to SAAS. The molecular weight values did not increase with increasing the SAAS contents (Table 3). It can be seen that CSWPU2 resin had the highest molecular weight, which also showed the lowest gloss level of film surface. Apart from the CSWPU3, the polydispersity of other CSWPU was very small. Below or above the optimum SAAS (50 % content, there was some detrimental effect on the molecular weight. When the SAAS content was lower than 50 % in the system, the molecular weight increased with the increase of the SAAS content. Because the SAAS served as the role of a chain-extending agent, the molecular weight of CSWPU resin increased in the chain extension step.

Table 3 Average molecular weight and polydispersity of the CSWPU films

Sample	Number average molecular weight (Mn)	Peak average molecular weight (Mp)	Weight average molecular weight (Mw)	Z-average molecular weight (Mz)	Polydispersity (PDI)
CSWPU1	40170	39298	52890	71316	1.31
CSWPU2	79692	92188	113219	163346	1.4
CSWPU3	16007	45745	64331	127904	4.0
CSWPU4	78274	84069	130800	234487	1.67

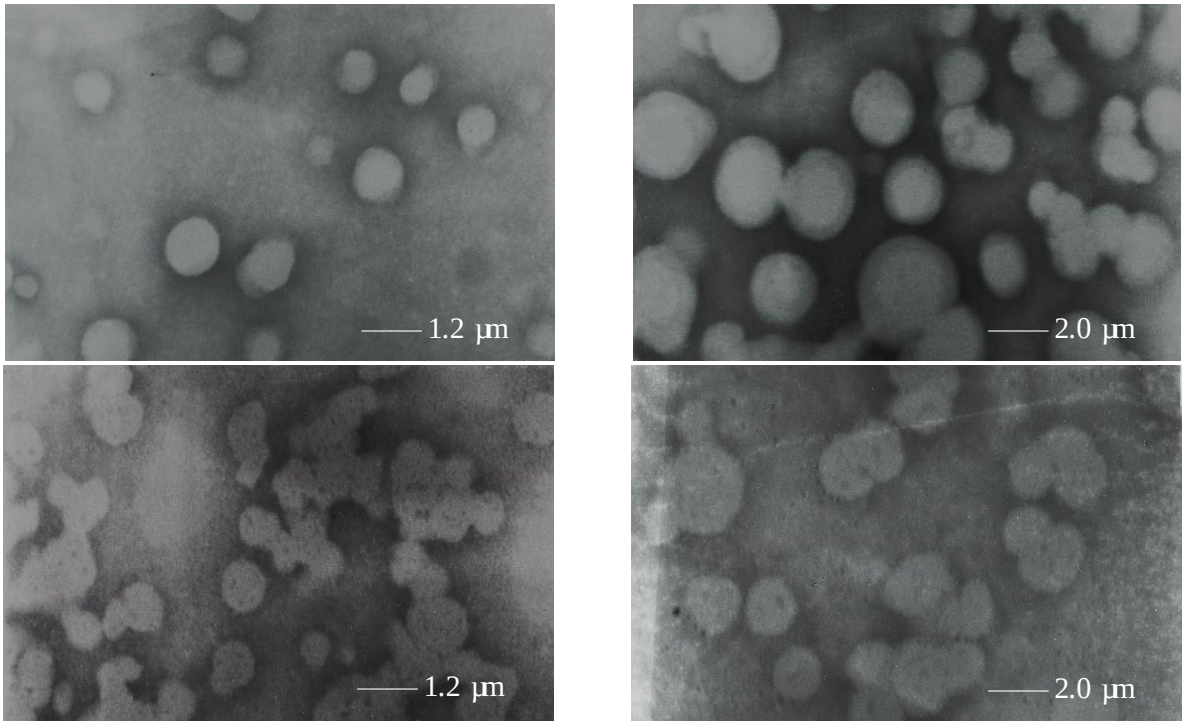

Figure 6. The TEM images of the CSWPU2 (upper) and CSWPU3 (lower) resin

Observations of latex particle morphology of CSWPU by TEM

In this part, the latex particle morphology was studied by TEM on resins of CSWPU2 and CSWPU3, respectively. From Figure 6, it is clear that the particle shape of two types of resins is of great difference. The latex particles of CSWPU2 resin were able to prevent from aggregating and disperse uniformly in a ball shape[29,30]. The edges of individual particles were clearly distinguishing, only very small particles showed a bit of aggregations. Nevertheless, the individual particles of CSWPU3 resin were very easy to aggregate and form clusters of macromolecular aggregates, and its appearance was nonspherical. In addition, it also can be seen that the average particle size of CSWPU2 was somewhat bigger than that of CSWPU3, this may explain why the matt effect of CSWPU2 resin was much better than that of CSWPU3 resin also identified by AFM analysis.

Swelling behaviour of CSWPU films

The swelling ratio of CSWPU films at ambient temperature is shown in Table 4. The CSWPU4 had the lowest swelling ratio (4 %) and its film's surface kept its original colour after being immersed. This could be due to the use of the soft segment with the molecular weight 2000. The final product had the highest molecular weight, which had been proved by GPC analysis. Each of the other three CSWPU films had various degrees of swelling ratio. Among them, the percentage of swelling of the CSWPU2 film was 13 % in deionized water, which had the best matt ability and the highest molecular weight. It is noticeable that the CSWPU films with good matting tended to have a higher molecular weight. Thus, the matt surfaces are typically harder and more resistant to water than glossy ones.

Table 4 Equilibrium swelling ratio (%) of the CSWPU films

Sample	Swelling ratio (%)	Colour change
CSWPU1	21	+
CSWPU2	13	+
CSWPU3	38	+
CSWPU4	4	–

Thermal analysis of CSWPU films by TGA

TGA analysis gave information not only on the thermal stability of CSWPU films, but also on their structure related to the degradative steps of diisocyanate and polyols, forming the polymer. The TGA and its DTG curves marked as a, b, c, and d in Figure. 7 correspond to the CSWPU1, CSWPU2, CSWPU3, and CSWPU4, respectively. The thermal degradation of CSWPU films started at about 250 °C. In the initial degradation stage, CSWPU2 had the highest degradative temperature at a 5 % weight loss compared with other three CSWPU films, which indicated that the CSWPU2 had more urea groups' contents than other three films. Because the first observable weight loss occurred through degradation of the urea and urethane groups in the hard segment, with the degradation rate of urethane groups being more rapid than that of urea groups[31]. From the perspective of molecular

structures, the first thermal decomposition step occurred in the hard segment could be explained by the electro-philic properties of the carbonyl groups. The form of (B) facilitated the transfer of hydrogen from the positively to the negatively charged nitrogen, followed by bond dissociation[32], causing the volatilization of diamine or other small molecules like the SAAS, etc.

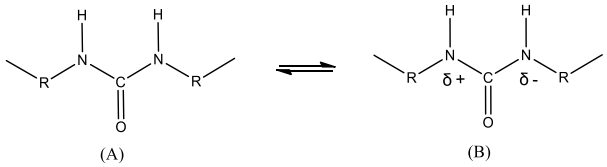

From another perspective, the decomposition of CSWPU was mostly influenced by the chemical structure of the component having the lowest bond energy[33]. Typically, the C-N bond energy was slower than the C-C bond energy, the C-N bonds in the rigid segments were more likely to degrade in the initial stage. The subsequent stages of degradation in the range of 300 ~ 420 °C occurred in the soft segments[31]. The last stage of the degradation process centred on a temperature of 420 ~450 °C was attributed to the gasification of any remaining organic components[34,35]. The amount of the final char yields above 500 °C was in the range of 1.3 ~ 3.5 % of the initial weight.

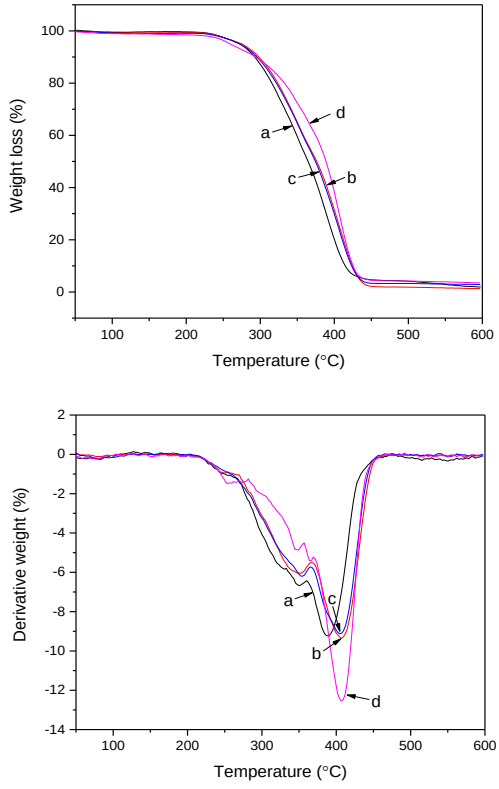

Figure 7. TGA and its DTG curves of CSWPU films

The derivative curves of all the analysed CSWPU show different stages of degradation:

(1) At approximately 250 ~ 300 °C, corresponding to the degradation of rigid segments formed by urethane and urea bonds;

(2) At 300 ~ 420 °C, corresponding to the degradation of soft segments;

(3) At 420 ~ 450 °C, corresponding to the gasification of any remaining organic components.

It is obvious that the temperature of the maximum degradative rate elevated from 390 °C to approximately 405 °C or above, as the SAAS content increased. This suggests that the increasing SAAS content could enhance the thermal stability to some extent. When compared the CSWPU4 film with other three CSWPU films, it had the largest rate of weight loss at the higher temperature 407 °C and upon 50 % weight loss, its thermal degradative temperature was also the highest. Thus it can be concluded that the increase in molecular weight of the soft segment enormously facilitated the improvement of thermal stability. All detailed data are listed in Table 5.

Table 5 Thermal properties of CSWPU films

Samples	T5% (°C)	T50% (°C)	Tmax (°C)	The final char yield (%)
CSWPU1	271	364	390	1.90
CSWPU2	275	376	407	1.29
CSWPU3	272	374	405	2.85
CSWPU4	259	388	407	3.49

T5%, T50% are the 5 % weight loss temperature and 50 % weight loss temperature, respectively. Tmax is the temperature of the maximum rate of weight loss.

Conclusions

In this paper, a combination of sulfonic and carboxylic hydrophilic chain-extending agents was employed to fabricate a novel CSWPU resin from a scientific water-based procedure. This kind of CSWPU resin was solvent-free and showed an excellent matt effect based on chemical extinction. The generation of spherical particles with diameter of 0.8 ~ 3.0 μm in the latexes, as well as on films, was responsible for the decrease of the gloss level of the surfaces. The matt effect was generated by the drying process of resin itself, without the additions of any matting agents. Moreover, the well matt CSWPU generally exhibited the high molecular weight, the low swelling ratio and good thermal stability. This research work is different from the conventional matt coatings based on physical extinction, it contributes to the further advancement of chemical matt techniques in matt coatings industry.

Acknowledgements

This research was performed as part of the program of the Intergration of Industry, Education and Research of Guangdong Province project (2011A091000007). The author gratefully acknowledge for supplying the financial support.

Notes and references

1 J. H. Wynne, P. a. Fulmer, D. M. McCluskey, N. M. Mackey and J. P. Buchanan, *ACS Appl. Mater. Interfaces*, 2011, **3**, 2005–2011.
2 F. Bauer, U. Decker, K. Czihal, R. Mehnert, C. Riedel, M. Riemschneider, R. Schubert and M. R. Buchmeiser, *Prog. Org. Coatings*, 2009, **64**, 474–481.
3 F. Bauer, U. Decker, S. Naumov and C. Riedel, *Prog. Org. Coatings*, 2014, **77**, 1085–1094.
4 F. Bauer, U. Decker, S. Naumov and C. Riedel, *Prog. Org. Coatings*, 2010, **69**, 287–293.
5 F. Bauer, R. Flyunt, K. Czihal, H. Langguth, R. Mehnert, R. Schubert and M. R. Buchmeiser, *Prog. Org. Coatings*, 2007, **60**, 121–126.
6 A. Larena and G. Pinto, 1993, **33**.
7 A. M. Sukhadia, D. C. Rohlfing, M. B. Johnson and G. L. Wilkes, *J. Appl. Polym. Sci.*, 2002, **85**, 2396–2411.
8 G. J. Vancsob, 1996, **3**.
9 Y. C. Du, S. L. Shi, C. Y. Bu, H. X. Dai, Z. G. Guo and G. Y. Tang, *Part. Sci. Technol.*, 2011, **29**, 368–377.
10 R. D. Hagenmaier, *PostharTest Biol. Technol.*, 2000, **19**, 147–154.
11 C. Amarante and N. H. Banks, *New Zeal. J. Crop Hortic. Sci.*, 2002, **30**, 49–59.
12 V. Kumar, N. Misra, J. Paul, Y. K. Bhardwaj, N. K. Goel, S. Francis, K. S. S. Sarma and L. Varshney, *Prog. Org. Coatings*, 2013, **76**, 1119–1126.
13 J. Ou, M. Zhang, H. Liu, L. Zhang and H. Pang, *J. Appl. Polym. Sci.*, 2015, **132**, 41707–41715.
14 M. Kunaver, *Dye. Pigment.*, 2003, **57**, 235–243.
15 V. D. Athawale and M. a. Kulkarni, *Prog. Org. Coatings*, 2009, **65**, 392–400.
16 M. Hirose, F. Kadowaki and J. Zhou, *Prog. Org. Coatings*, 1997, **31**, 157–169.
17 D. Kukanja, J. Golob and a Zupanc, *J. Appl. Polym. Sci.*, 2000, **78**, 67–80.
18 U. Šebenik, J. Golob and M. Krajnc, *Polym. Int.*, 2003, **52**, 740–748.
19 P. Kang, W. Song, J. Hui, W. Chen and R. Yan, *Paint Coatings Indust.*, 2010, **40**, 52–55.
20 X. Li, X. Wu, S. Wu, Z. Jia and N. Cao, *Paint Coatings Indust.*, 2010, **40**, 30–32.
21 W. Yang, J. Yang, Q. Wu, J. Zhang and M. Wu, *Polyurethane Indust.*, 2012, **27**, 1–4.
22 M. M. Rahman, A. Hasneen, I. Chung, H. Kim, W.-K. Lee and J. H. Chun, *Compos. Interfaces*, 2013, **20**, 1–12.
23 S. Zhang, H. Lv, H. Zhang, B. Wang and Y. Xu, *J. Appl. Polym. Sci.*, 2006, **101**, 597–602.
24 L. Zhai, R. Liu, F. Peng, Y. Zhang, K. Zhong, J. Yuan and Y. Lan, *J. Appl. Polym. Sci.*, 2013, **128**, 1715–1724.
25 W. Li, Y. Wu, W. Liang, B. Li and S. Liu, *Appl. Mater. interfaces*, 2014, **6**, 5726–2734.
26 C. Zhang, D. Vennerberg and M. R. Kessler, *J. Appl. Polym. Sci.*, 2015, **132**, n/a–n/a.
27 M. M. Rahman, H.-D. Kim and W.-K. Lee, *J. Adhes. Sci. Technol.*, 2009, **23**, 177–193.
28 Y. He, X. Zhang, X. Zhang, H. Huang, J. Chang and H. Chen, *J. Ind. Eng. Chem.*, 2012, **18**, 1620–1627.
29 C. Wu, J. Huang, Y. Wen, S. Wen, Y. Shen and M. Yeh, *J. Chinese Chem. Soc.*, 2009, **56**, 1231–1235.
30 E. Princi, S. Vicini, K. Castro, D. Capitani, N. Proietti and L. Mannina, *Macromol. Chem. Phys.*, 2009, **210**, 879–889.
31 T.-L. Wang and T.-H. Hsieh, *Polym. Degrad. Stab.*, 1997, **55**, 95–102.
32 J. Ferguson and Z. Petrovic, *Eur. Polym. J.*, 1976, **12**, 177–181.
33 F. M. B. Coutinho and M. C. Delpech, *Polym. Degrad. Stab.*, 2000, **70**, 49 – 57.
34 Y. Li, B. a J. Noordover, R. a T. M. Van Benthem and C. E. Koning, *Eur. Polym. J.*, 2014, **52**, 12–22.
35 X. J. Li, D. X. Sun and Y. H. Zhang, *J. Polym. Res.*, 2014, **21**.

Graphical abstract

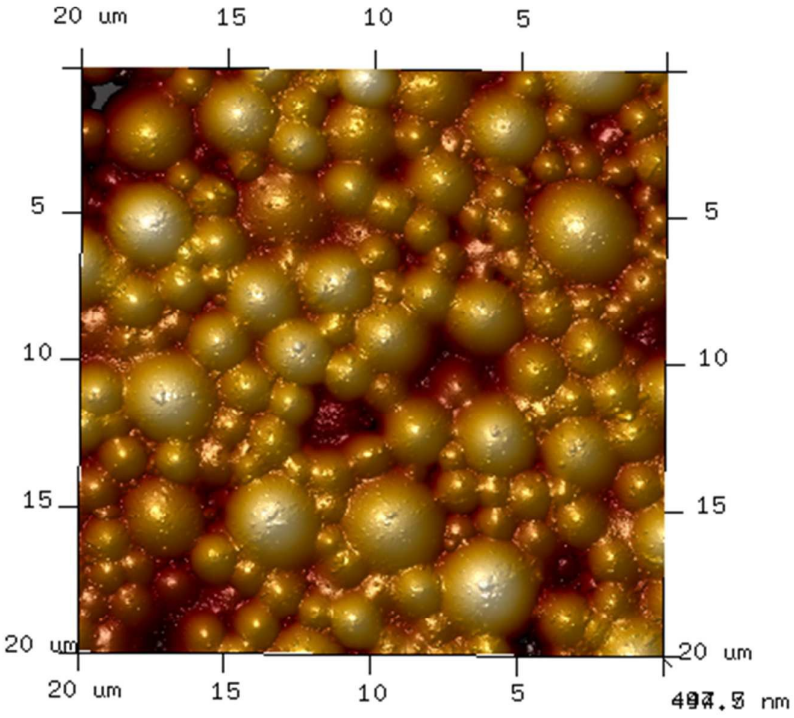

A sentence: self-extinction and solvent-free waterborne polyurethane resin without the addition of extra matting agents.